 FDMP, vol.5, no.2, pp.161-175, 2009

Determination of Physical Properties of Porous Materials by a Lattice Boltzmann Approach

M.R. Arab[1,2], E. Semma[3], B. Pateyron[1] and M. El Ganaoui[1]

Abstract: In this work, flows in porous media are simulated by using a Lattice Boltzmann Method (LBM). A model D2Q9 with a single collision operator is proposed. This method is applied on 2D digital images obtained by a Scanning Electron Microscope technique (SEM), and followed by a special treatment in order to obtain an image of synthesis that is finally read by the numerical code. The first results tested on two-dimensional configurations show the reliability of this strategy in simulating with a good accuracy phenomena of heat and mass transport. The numerical study is extended to the prediction of physical parameters that characterize a porous material (in particular, permeability that can be hardly estimated experimentally).

Keywords: Lattice Boltzmann Method, porous media, permeability, heat and mass transfers.

1 Introduction

Prediction of physical properties of porous materials is of crucial importance when dealing with industrial applications in the field of thermal coating processes [Dyshlovenko 2006].

It is expensive and time consuming to make direct experimental measurements besides of difficulties due to the thickness of the coatings (few till 100 micrometers) and the related inhomogeneous porosity.

In these days, thanks to the development in the realm of computer industry and science (especially in instrumentations and techniques like scanning electronic microscopy (to obtain 2D pictures) and micro computer tomography (to obtain 3D

[1] SPCTS, FST Limoges, France

[2] This paper is submitted as a contribution to a special issue of FDMP for the ICTEA-2007 proceedings

[3] LM, FST, Settat, Maroc

pictures) to scan medium microstructures) a numerical simulation is becoming a serious alternative to estimate the physical properties of such complex media.

For the case of flow simulations through porous media one can find in the literature grid-based methods as finite difference finite volumes or finite-element approaches. These methods suffer sometimes difficulties in the implementation of the boundary conditions. This is not the case, however, for the Lattice Boltzmann Method (LBM) proposed in the present work.

In the last few years, this promising mesoscopic method has proven efficient for the simulation of classical fluid flows including flows through porous media [Succi 2001; Sukop 2006; Mohamad 2007]. The main advantages of this tool are the efficiency in parallel computing, and using simple expressions to describe boundary conditions [He and Luo, 1997a; Dupuis 2002; Evgrafov, Pingen and Matue, 2006]. This tool is also considered convenient for the simulation of heat transfer problems [Chen and Doolen 1998; Zhang and Chen 2003] and also when phase change is involved [Semma, ElGanaoui and Bennacer 2008].

In this paper, a short description of this technique is presented. A D2Q9 model with nine velocity vectors in a square lattice is used and validated with respect to the *Poiseuille* flow (classical solution). The LBM is applied then to simulate a single phase flow through a porous structure using binary images. Applying Darcy's law for low velocity flows, the permeability of the domain is estimated. Derivation of a close method to treat thermal problems is under progress.

2 Formulation of lattice Boltzmann methods

Historically, LBM evolved from the Boolean Lattice Gas Automata (LGA). Also it can be derived from the Boltzmann equation. One can see the works of He and Luo (1997) for more details.

The essential point in this method is the particle distribution function (PDF) f attributed to every node in the domain to be studied. This function gives the probability in uniformly spaced lattice to find a fluid particle with a lattice velocity u at a position x and time t.

In the present development, The LB model comprises two distribution functions, f and g, for the flow field and the temperature field, respectively. The density and the temperature distribution functions, f and g, are defined as the probability of particles at site x and time t moving with the particle velocity c_α during the time step δt in each lattice direction (link) α. The same model was proposed by [Barrios et *al.* 2005, Yu et al. 2002]. The two distribution functions obey to their respective lattice Boltzmann transport equations to the single relaxation Bhatnagar–Gross–Krook (BGK) approximation.

2.1 LBM for hydrodynamic Equation

Without focusing on details which are easily found in the work of Mezrhab, Bouzidi and Lallemand (2004), the discrete form of the Boltzmann equation for a single phase flow is produced by the approximation of Bhatnagar-Gross-Krook (BGK) [Yu, Luo and Girimaji 2002; Succi, 2001; Mohamad, 2007]:

$$f_\alpha(x+e_\alpha\delta t, t+\delta t) - f_\alpha(x,t) = \Omega \tag{1}$$

Here e_α is the microscopic lattice velocity at lattice node x at time t where the space and time steps are set to the unity. Ω is the collision operator which represents the variation of the PDF due to the inter-particles collisions. This operator is given by:

$$\Omega = -\frac{1}{\tau_v}\left[f_\alpha(x,t) - f_\alpha^{eq}(x,t)\right] \tag{2}$$

τ_v is defined as the dimensionless relaxation time of the collision, and f^{eq} is the Equilibrium Particle Distribution Function (EPDF) defined by the Boltzmann-Maxwell equation:

$$f^{eq} \equiv \frac{\rho}{(2\pi RT)^{D/2}} \exp\left(-\frac{(e-u)^2}{2RT}\right) \tag{3}$$

And for a D2Q9 model shown in Fig. 1, this function can be written as:

$$f_\alpha^{eq} = w_\alpha \rho \left[1 + \frac{(e_\alpha.u)}{c_s^2} + \frac{(e_\alpha.u)^2}{2c_s^2} - \frac{uu}{2c_s^2}\right] \tag{4}$$

with w_α being the directional weights of the PDF:

$$w_0 = \frac{4}{9}, \quad w_{1,2,3,4} = \frac{1}{9}, \quad w_{5,6,7,8} = \frac{1}{36} \tag{5}$$

which conserve the lattice isotropy [Dupuis, 2002]. c_s is calculated as: $c_s = 1/\sqrt{3}$
By applying the Chapman-Enskog expansion to the Lattice Boltzmann equation (1) to recover the steady-state Navier-Stokes equations, density and momentum at each fluid node are calculated by these relations:

$$\rho = \sum_\alpha f_\alpha(x,t) = \sum_\alpha f_\alpha^{eq} \tag{6}$$

$$\rho u(x,t) = \sum_\alpha e_\alpha f_\alpha(x,t) = \sum_\alpha e_\alpha f_\alpha^{eq} \tag{7}$$

where ρ is the fluid mass density and u is the fluid macroscopic speed. The internal energy can also be expressed as:

$$\begin{aligned}\rho\varepsilon(x,t) &= \frac{1}{2}\sum_{\alpha}(e_\alpha - u(x,t))^2 f_\alpha(x,t) \\ &= \frac{1}{2}\sum_{\alpha}(e_\alpha - u)^2 f_\alpha^{eq}\end{aligned} \tag{8}$$

where $\varepsilon(x,t) = \frac{D}{2}T$.

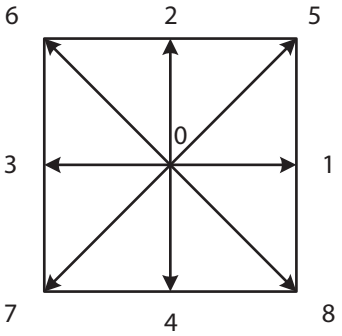

$$e_\alpha = \begin{cases}(0,0) & \alpha = 0 \\ (\pm 1,0),(0,\pm 1) & \alpha = 1,2,3,4 \\ (\pm 1,\pm 1) & \alpha = 5,6,7,8\end{cases}$$

Figure 1: A D2Q9 LBM model with its 9 lattice velocity vectors

The lattice kinematics viscosity in the flow domain is obtained by:

$$\upsilon = c_s^2(\tau_v - 0.5) \tag{9}$$

Then υ will depend only on the relaxation time. The pressure is obtained through an equation of state:

$$p = \rho c_s^2 \tag{10}$$

while the traditional solvers of Navier-Stokes equations need to solve the Poisson equation [Al-Zoubi, 2006]

2.2 LBM for energy equation

The evolution equation for the internal energy is given as follows:

$$g_i(x+c_i\Delta t, t+\Delta t) - g_i(x,t) = -\frac{1}{\tau_T}(g_i(x,t) - g_i^{eq}(x,t)) \tag{11}$$

Where g_α is the energy distribution function, τ_T is the dimensionless relaxation time for the temperature field, and the equilibrium temperature distribution function is given by:

$$g_0^{eq} = -\frac{2}{3}\rho e\frac{\mathbf{u}.\mathbf{u}}{2c^2} \tag{12}$$

$$g_{k=1,2,3,4}^{eq} = \frac{\rho e}{9}\left(\frac{3}{2} + \frac{3}{2}\frac{\mathbf{c_k}.\mathbf{u}}{c^2} + \frac{9}{4}\frac{(\mathbf{c_k}.\mathbf{u})^2}{c^4} - \frac{3}{2}\frac{\mathbf{u}.\mathbf{u}}{c^2}\right) \tag{13}$$

$$g_{k=5,6,7,8}^{eq} = \frac{\rho e}{36}\left(3 + 6\frac{\mathbf{c_k}.\mathbf{u}}{c^2} + \frac{9}{2}\frac{(\mathbf{c_k}.\mathbf{u})^2}{c^4} - \frac{3}{2}\frac{\mathbf{u}.\mathbf{u}}{c^2}\right) \tag{14}$$

The macroscopic temperature is calculated from the internal energy as:

$$\rho\varepsilon = \sum_\alpha g_\alpha \tag{15}$$

The temperature and internal energy are related through the state equation $e = RT$. The Chapman-Enskog expansion for the density distribution function recovers the macroscopic energy equation. This gives the thermal diffusivity α_T in term of the single relaxation:

$$\alpha_T = \frac{1}{3}\left(\tau_T - \frac{1}{2}\right)c^2\delta t \tag{16}$$

3 Porous Media

The single-phase steady-state incompressible flow through a porous media is defined by Darcy's law:

$$\langle u' \rangle = -\frac{k'}{\mu'}\nabla p' \tag{17}$$

where the factor k' is introduced as the permeability coefficient which determine the ability of the domain to allow the fluid to pass through it. Here $\langle u' \rangle$ is the mean rate of the fluid flux at the outlet, $\nabla p'$ is the pressure drop along the domain length and $\mu' = \rho'\upsilon'$ is the viscosity of the fluid.

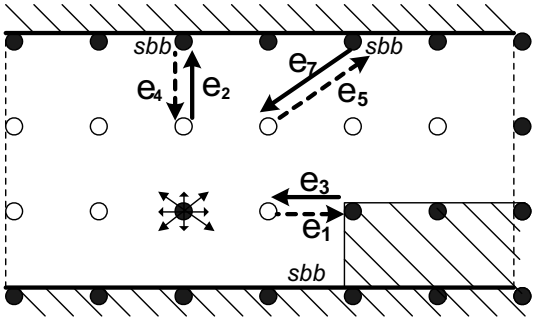

Figure 2: Simple implementation of SBB in a porous media. Hollow circles are fluid nodes and the others are obstacles (solids)

For small domains, porous media is introduced in the model by defining solid nodes as obstacles. A Standard Bounce Back condition (SBB) is applied at these obstacles. With such condition, after collision, incident fluid particles are sent back to lattice nodes they came from. This condition described in Fig. 2 also ensures the no-slip condition at surface boundaries of the domain.

For large domains (in cm), one can refer to the work of Dardis and McKloskey (1998) in which they introduce for each lattice node a new parameter n_s ranging between 0 (for the totally fluid node) and 1 (for the totally solid node).

4 Flow Simulations

4.1 Validations

4.1.1 Poiseuille flow

Numerical simulations for the plane Poiseuille flow driven by either a pressure gradient or a fixed velocity profile at the entrance of channel have been carried out to test the validity of the incompressible LBM model.

The algorithm used in this work for the simulation is described as follows:

- initialize the problem: setting the lattice size and reading fluid/obstacles nodes. Apply the initial and boundary conditions to calculate the unknown variables of the lattice.
- compute the hydrodynamic mass density and macroscopic velocity from equations (6,7).
- Calculation of the EPDF from Eq.(4).

- Application of collide/stream steps according to Eq.(1).

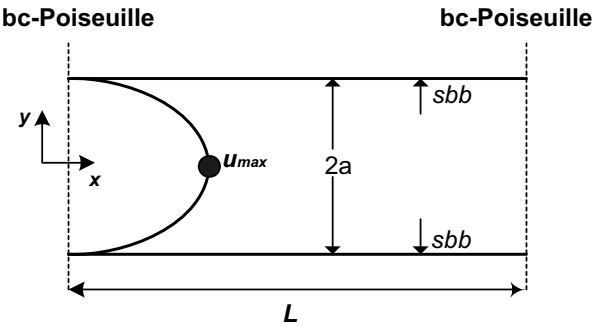

Figure 3: The geometry of the studied canal. A lattice of 200×50 pixels is used for the LBM simulation.

Following these steps we have first tested the code on a simple two-dimensional *Poiseuille* configuration, as shown in Fig. 3. The analytic solution for velocity of this flow is:

$$u_x = \frac{\Delta p}{2\mu L}\left(a^2 - y^2\right) \tag{18}$$

where $u_x = 0$ at $y = \pm a$, $u_{\max} = \frac{3}{2}u_{ave}$ at $y = 0$ and the pressure drop $\Delta p = p_{in} - p_{out}$ are the boundary conditions.

The solution of equation (18) for a given mean velocity agrees with a parabolic velocity profile (see Fig. 4).

We carried out LB simulations on 200x50 lattice grid points. For achieving a steady state regime the following convergence criteria is considered:

$$\frac{\sum_{i,j}\left|u_{ij}^{(n+1)} - u_{ij}^{(n)}\right|}{\sum_{i,j}\left|u_{ij}^{(n+1)}\right|} \leq 10^{-6} \tag{19}$$

where n is the number of time steps, i and j index to the x and y coordinates.

Our simulations show that the velocity profile remains unchanged (as a parabolic profile) along the channel (fig. 4) and that the pressure distribution is linear along the channel and uniform across it. All these results are in excellent agreement with the analytical solutions of the Navier-Stokes equation.

This agreement validates the capacity of this tool to simulate with high precision flows through porous media.

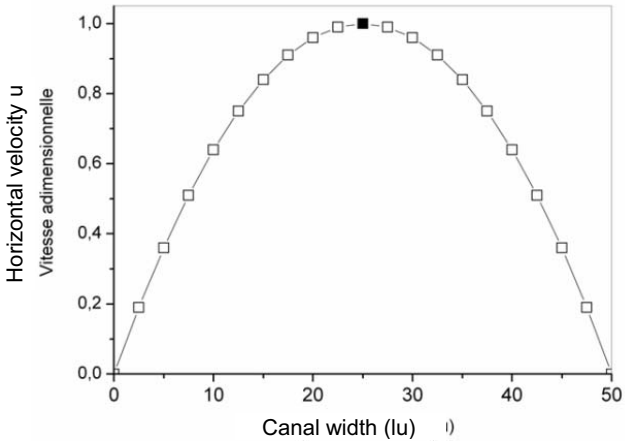

Figure 4: The horizontal velocity profile of Poiseuille flow. Comparison between the analytical solution (continuous) and LBM simulation results (squares), (*lu*: lattice unit).

Table 1: Present numerical values with uniform mesh 150×150 for $Ra = 10^3$ to 10^5 and 200×50 for $Ra = 10^6$, and underlines reference values (de Vahl Davis, 1983).

Ra	$u_{\max}$		$v_{\max}$		Nu	
10^3	3.699	3.695	3.650	3.644	1.116	1.117
10^4	19.620	19.611	16.178	16.172	2.245	2.246
10^5	68.68	68.62	34.73	34.725	4.521	4.522
10^6	220.418	219.20	64.763	64.621	8.814	8.814

4.1.2 Natural convection

We verify the applicability of the developed LBM for the calculation of natural convection. The simulation is restricted to two-dimensional thermal fluid dynamics in a square cavity with isothermal vertical walls and adiabatic horizontal walls.

The temperature difference between the sidewalls introduces buoyancy (that can be modeled on the basis of the Boussinesq approximation).

The Prandtl number is fixed to $Pr = 0.71$ and Rayleigh numbers is varied from $Ra = 10^3$ to $Ra = 10^6$.

LB solution produces the expected behaviors for low and high Rayleigh numbers. Table 1 summarizes representative quantities of the flow field and heat transfer. Good agreement is found between LB results and classical based Navier Stokes

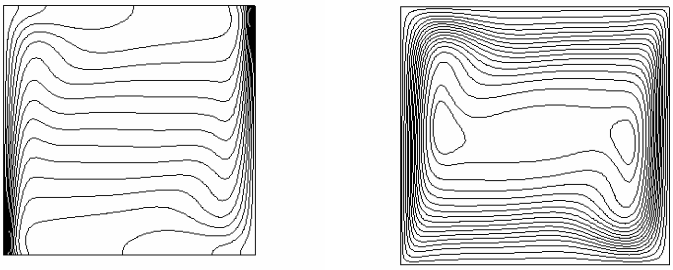

Isotherms Streamlines

Figure 5: Isotherms and Streamlines for $Ra = 10^6$.

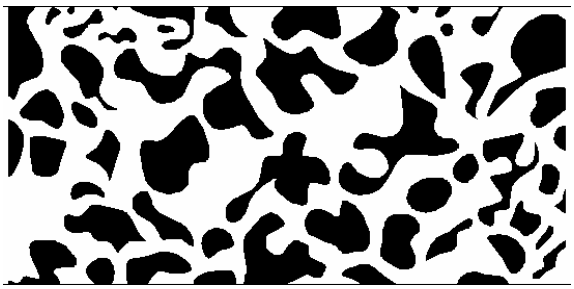

Figure 6: Binary image of porous media. White zones are fluid domains and black ones are the solids. A lattice of 552×276 pixels is used for the LBM simulations.

simulations (de Vahl Davis, 1983).

The heat transfer at the hot surface increases with Ra. At $Ra > 10^5$, the flow is characterised by distinct boundary layers adjacent to the vertical heated walls. An illustration of the temperature and flow patterns LB resulting is given on the figure 5 for $Ra = 10^6$.

4.2 Simulation of flow through porous media

For the purpose to simulate the flow through a porous medium, the binary image in Fig. 6 has been considered. This image was taken by a Scanning Electron Microscope (SEM), considered for a non-destructive investigation, for a pattern in silicon wafer [see *COMSOL Multiphysics* Library for the original image] then treated so that fluid and solid zones could be distinguished. This example was studied numerically by using a a finite element method through the *COMSOL Multiphysics* tool. The size of the domain is 552×276pixels with a characteristic length of 640

micron. This implies a lattice spacing $\Delta x = 1.16$ microns leading to a low Knudsen number of the order of 10^{-2} which supports the assumption that the LBM is approximating the Navier-Stokes equation.

To simulate the flow (water is considered as the work fluid), the initial conditions in the simulation have been set as $u = 0$ for the flow velocity, and $\rho = 1$ for the fluid density in the whole domain. The relaxation time is set to 1 then the kinematic viscosity is calculated.

The boundary conditions for the flow are uniform density at the inlet/outlet where the pressure boundary conditions are maintained by imposing $\rho_{in} > \rho_{out}$ with zero velocity within the domain (so that a single phase fluid enters from the inlet (left) and flows towards the outlet (right)).

The unknown variables at the inlet/outlet boundaries are calculated from the relations in Tab. 2 depending on equations (6, 7) for the density and velocity and on figure 1 to determine directions and values of the unknown PDFs. Besides, the no-slip boundary conditions are implemented at the top and bottom surfaces. We can refer here to the book of Sukop and Thorne (2006) for additional details.

Table 2: inlet/outlet pressure boundary conditions

inlet	
known	unknown
ρ_{in}, f_0, f_3, f_2 f_4, f_6, f_7	$u_x = \rho_{in} - (f_0 + f_2 + f_4 + 2(f_3 +$ $f_6 + f_7))$
	$f_1 = f_3 + \frac{2}{3}u_x$
	$f_5 = f_7 + \frac{1}{2}(f_4 - f_2) + \frac{1}{6}u_x$
	$f_8 = f_6 + \frac{1}{2}(f_2 - f_4) + \frac{1}{6}u_x$
outlet	
known	unknown
ρ_{in}, f_0, f_1, f_2 f_4, f_5, f_8	$u_x = -\rho_{out} + (f_0 + f_2 + f_4 +$ $2(f_1 + f_5 + f_8))$
	$f_3 = f_1 - \frac{2}{3}u_x$
	$f_7 = f_5 + \frac{1}{2}(f_2 - f_4) - \frac{1}{6}u_x$
	$f_6 = f_8 + \frac{1}{2}(f_4 - f_2) - \frac{1}{6}u_x$

The dimensionless permeability, which characterizes the porous media, is calculated from Eq.(17) by replacing each variable with its corresponding relation from Tab. 3. This gives:

$$k = \frac{k'}{L^2} = \frac{\rho u^2}{Re \Delta p} \tag{20}$$

Here u is the dimensionless mean velocity over all the fluid nodes.

Figure 7 presents contours of velocity field for three different grids. We note that the behavior of the fluid does not change much and that a grid of 276×138 makes it possible to deal with this problem with an acceptable accuracy.

Table 3: definition of the non dimensional variables

$\Delta x = L/N$	$\upsilon' = \upsilon(\Delta x^2/\Delta t)$
$\Delta t = (c_s/c'_s)\Delta x$	$\rho' = (\rho \Delta m)/\Delta x^3$
$u' = u(\Delta x/\Delta t)$	$\Delta p' = (\Delta p \Delta m)/(\Delta x \Delta t^2)$

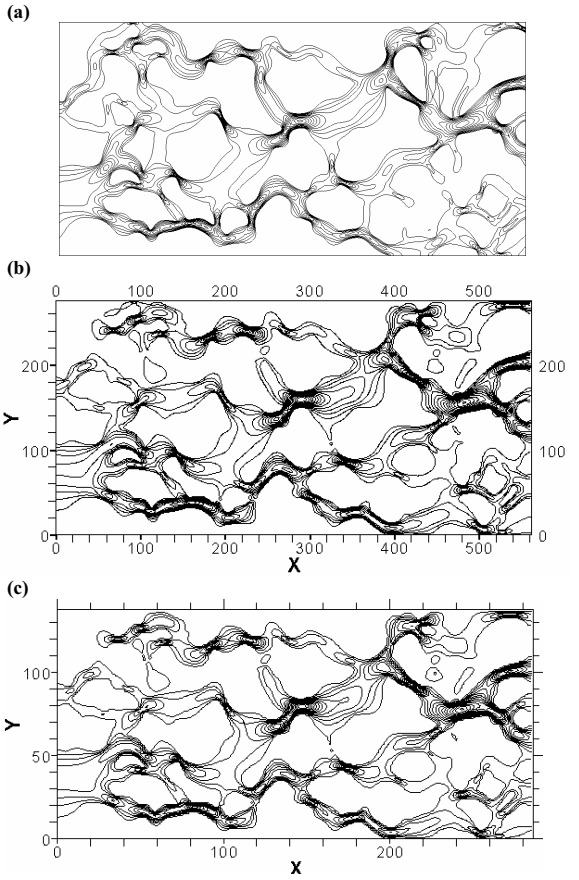

Figure 7: Contours of horizontal velocity field (a) *COMSOL Multiphysics* computations, (b) LBM-D2Q9 model for 552×276 pixels lattice and (c) LBM-D2Q9 model for 276×138 pixels lattice.

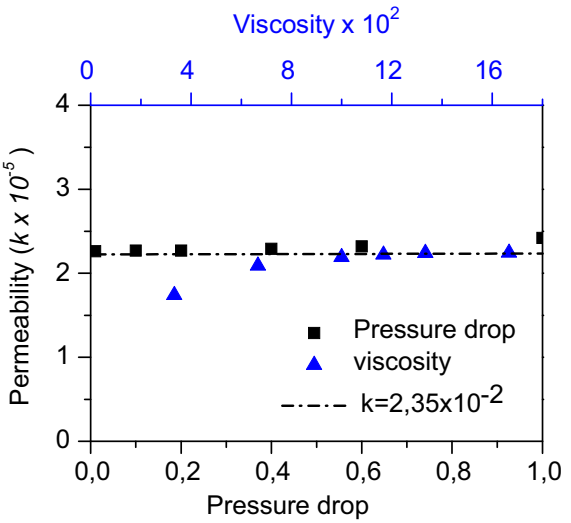

Figure 8: Variation of the permeability versus the lattice pressure drop and lattice viscosity.

In figure 8, the permeability variations have been plotted versus the pressure (density) gradient and the lattice viscosity. We can see from this figure that the permeability varies around a mean value ($k = 2,35 \times 10^{-5}$) which can be considered as the dimensionless value of the permeability for this geometry. This value is practically independent of the viscosity of the fluid saturating the pores of the porous medium and then k is viscosity independent.

5 Conclusion

In this work, flow in porous media has been simulated by using a Lattice Boltzmann method (LBM). A D2Q9 model with a single collision operator has been proposed.

This method has been applied on 2D digital images obtained by a Scanning Electron Microscope (SEM), and further treated to obtain a synthesis image to be read (pixel by pixel) by a numerical code.

The first results for a two-dimensional configuration have shown the aptitude of this method to simulate with very good accuracy the phenomena of interest.

The numerical study has been also extended to the simulation of physical parameters that characterize porous materials, like relative permeability (which is difficult to investigate experimentally). Remarkably, the permeability has been deducted directly from the picture.

Acknowledgement: First author would like to thank Dr. A. A. Mohamad and also Dr. R. Bennacer for fruitful discussions during their stay in Limoges last summer.

Nomenclature

D	dimension of the model
T	temperature, K
P	pressure Pa
$f(x,t)$	particle distribution function (LBM)
$f_{eq}(x,t)$	equilibrium particle distribution function (LBM)
$g(x,t)$	thermal particle distribution function (LBM)
$g_{eq}(x,t)$	Thermal equilibrium particle distribution function (LBM)
t	time
R	constant of ideal gas
u	fluid macroscopic velocity (LBM)
e	lattice velocity vector
c_s	"pseudo" speed of sound in the lattice system (LBM)
L	lattice size (LBM)
k	Permeability m^2

Greek Symbols

μ	dynamic viscosity, $Pa.s$
ρ	mass density, kg/m^3
τ	relaxation time (LBM)
w	weight associated with lattice vector direction
υ	kinematics viscosity
ε	internal energy
α_T	thermal diffusivity m^2/s
δ	time/space step
α	lattice index

Exponents

n time steps number (LBM)

‘ dimensioned variable

Non-dimensional Numbers

Ra Rayleigh number
Re Reynolds number
Pr Prandtl number
Kn Knudsen number
Nu Nusselt number

References

Al-Zoubi A. (2006): Numerical Simulations of Flows in Complex Geometries Using the Lattice Boltzmann Method, *Doctoral Thesis*. Clausthal Germany.

Barrios G.; Rechtman R.; Rojas J.; Tovar R. (2005): The lattice Boltzmann equation for natural convection in a two-dimensional cavity with a partially heated wall, *J. Fluid Mech.* Vol. 522, pp.91-100.

Chen S.; Doolen G. (1998): Lattice Boltzmann Method for Fluid Flow. *Annu. Rev. Fluid Mech.* Vol. 30, pp.29-64.

COMSOL Multiphysics 3.2 Package: *Earth Science Module. Model Library*.

Dardis O.; McCloskey J. (1998): Lattice Boltzmann scheme with real numbered solid density for the simulation of flow in porous media. *Phys. Rev. E* Vol. 57, pp. 4834-4837.

De Vahl Davis G. (1983): Natural Convection of air in a Square Cavity. A Bench Mark Numerical Solution. *Int. J. Numerical Methods in Fluids* Vol. 3, pp. 249-264.

Dupuis A. (2002): From a lattice Boltzmann model to a parallel and reusable implementation of a virtual river. *Doctoral Thesis*. Geneva Switzerland.

Dyshlovenco S.; Paulowski L.; Pateyron B.; Smurov I.; Harding J. H. (2006): Modeling of plasma particle interactions and coating growth of plasma spraying of hydroxyapatite, *Surface & coatings Technology,* Vol. 200, pp. 3757-3769.

Evgrafov A.; Pingen G.; Matue K. (2006): Topology optimization of fluid problems by the lattice Boltzmann method. *University of Colorado USA*.

He X.; Luo Li-Shi. (1997a): Theory of the lattice Boltzmann method: From the Boltzmann equation to the lattice Boltzmann equation. *Phys. Rev. E* Vol. 56, pp. 6811-6817.

He X.; Luo Li-Shi. (1997b): A priori derivation of the lattice Boltzmann equation. *Phys. Rev. E* Vol. 55, pp. R6333-R6336.

Mezrhab A.; Bouzidi M.; Lallemand P. (2004): Hybrid lattice-Boltzmann finite-difference simulation of convective flows, *Computers & Fluids* Vol. 33, pp. 623-641.

Mohamad A.A. (2007): Applied Lattice Boltzmann Method for Transport Phenomena, Momentum, Heat and Mass Transfer. Calgary-Canada.

Semma E.; El Ganaoui M.; Bennacer R.; Mohamad A.A. (2008): Investigation of flows in solidification by using the lattice Boltzmann method, *International Journal of Thermal Sciences* Vol. 47, pp. 201-208.

Succi S. (2001): The Lattice Boltzmann Equation for Fluid Dynamics and Beyond. *Oxford Science Publications*.

Sukop M.; Thorne D. (2006): Lattice Boltzmann Modeling: An Introduction for Geoscientists and Engineers. *Springer Publications*.

Yu H.; Luo L.S.; Girimaji S.S. (2002): Scalar mixing and chemical reaction simulations using lattice Boltzmann method, *Int. J. Comp. Eng. Sci.* Vol. 3 No. 1, pp. 73-87.

Zhang R.; Chen H. (2003): Lattice Boltzmann method for simulations of liquid-vapor thermal flows. *Physical review E* Vol. 67, pp. 066711.